

# Electron–positron annihilation into four charged pions and the $a_1\rho\pi$ Lagrangian\*

Peter Lichard<sup>1,2</sup> and Josef Juráň<sup>1</sup>

<sup>1</sup>*Institute of Physics, Silesian University in Opava, Bezručovo nám. 13, 746 01 Opava, Czech Republic*

<sup>2</sup>*Institute of Experimental and Applied Physics, Czech Technical University, Horská 3/a, 120 00 Prague, Czech Republic*

(Dated: May 14, 2018)

The excitation curve of  $e^+e^-$  annihilation into four charged pions in the  $\rho(770)$  region is calculated using three existing models with  $\rho$  mesons and pions in intermediate states supplemented by Feynman diagrams with the  $a_1(1260)\pi$  intermediate states. A two-term phenomenological Lagrangian of the  $a_1\rho\pi$  interaction is used. The mixing angle is determined by fitting the  $e^+e^- \rightarrow \pi^+\pi^-\pi^+\pi^-$  cross section data of the Novosibirsk CMD-2 collaboration and also its combination with the low-energy part of the BaBar collaboration data. It is shown that the inclusion of the  $a_1\pi$  intermediate states succeeds in obtaining a good agreement with the data on both cross section and the  $\rho^0 \rightarrow \pi^+\pi^-\pi^+\pi^-$  decay width. When moving to energies above 1 GeV, the  $\rho(1450)$  and  $\rho(1700)$  resonances are taken into account to get excellent agreement with the BaBar data over the full energy range up to 4.5 GeV.

PACS numbers: 13.30.Eg, 13.66.Bc, 12.39.Fe, 13.25.Jx

## I. INTRODUCTION

Task of describing the excitation curve of the  $e^+e^- \rightarrow \pi^+\pi^-\pi^+\pi^-$  reaction at low energies is closely related to the investigation of the energy dependent decay width of the four pion decay of  $\rho(770)$ . The validity of the factorization of the cross section into the  $\rho(770)$  production and decay parts is generally assumed on the basis of the vector meson dominance (VMD) hypothesis [1]. The assumption of factorization allows experimentalists to determine a particular partial decay width at the nominal  $\rho(770)$  mass on the basis of measurement the  $e^+e^-$  annihilation cross section into the corresponding final state at the corresponding energy. The current experimental value  $\Gamma(\rho^0 \rightarrow \pi^+\pi^-\pi^+\pi^-) = (2.8 \pm 1.4 \pm 0.5)$  keV was obtained in that way [2]. In this work, we will also assume a one-to-one correspondence between the cross section and the energy dependent decay width at the same energy, ignoring the complications which may appear if some conditions are not met [3]. Needless to say that the evaluation of the decay width is less demanding technically and computationally than that of the cross section (five-dimensional quadrature instead of eight-dimensional one in the case of four-body final states).

The cross section of the  $e^+e^-$  annihilation into the  $2\pi^+2\pi^-$  and  $\pi^+\pi^-2\pi^0$  final states was considered by Decker, Heiliger, Jonsson, and Finkemeier [4] in conjunction with the CVC-related decays of the  $\tau$  lepton. The intermediate states of their model contained  $\rho(770)$ ,  $a_1(1260)$ , and a scalar-isoscalar two-pion resonance. In the two-charged-two-neutral case also the  $\omega(782)$  was included. The  $a_1\rho\pi$  vertex factors were adopted from the study of the three-pion decay of the  $\tau$  lepton by Isgur, Morningstar, and Reader [5]. Czyż and Kühn [6] constructed a Monte Carlo generator of the reaction  $e^+e^- \rightarrow \gamma + 4\pi$ . The hadronic matrix elements were used in the form suggested in [4], corrected only for some minor deficiencies. To check the soundness of their approach, Czyż and Kühn calculated also the excitation curves of the nonradiative reactions  $e^+e^- \rightarrow \pi^+\pi^-\pi^+\pi^-$  and  $e^+e^- \rightarrow \pi^+\pi^-2\pi^0$  in qualitative agreement with available data. Ecker and Unterdorfer [7, 8] performed the first calculation of the processes  $e^+e^- \rightarrow 4\pi$  and  $\tau \rightarrow \nu_\tau 4\pi$  with the correct structure to  $O(p^4)$  in the low energy expansion of the Standard Model extrapolated to the resonance region. To get a good description of the  $e^+e^- \rightarrow \pi^+\pi^-\pi^+\pi^-$  cross section up to 1 GeV, they had to include as additional contribution the  $a_1$  exchange. They circumvented the  $a_1\rho\pi$  Lagrangian ambiguity by choosing a special relation among the individual coupling constants.

The four-pion decays of the  $\rho(770)$  are generally considered a convenient test ground of the low-energy effective theories of the interactions of  $\rho$  mesons and pions. In the past, several papers appeared that calculated the corresponding partial decay widths [9–13]. Moreover, Achasov and Kozhevnikov [12, 13] argued that the four-pion decay widths of  $\rho(770)$  are not experimentally well defined because they require the averaging over a mass interval in which they rise rapidly. They therefore calculated, in addition to the decay widths  $\Gamma(\rho^0 \rightarrow \pi^+\pi^-\pi^+\pi^-)$ ,  $\Gamma(\rho^0 \rightarrow \pi^+\pi^-\pi^0\pi^0)$ ,

---

\*This paper is dedicated to the late Julia Thompson, who drew the attention of one of us (P. L.) to the experimental program of the Budker Institute of Nuclear Physics at Novosibirsk.

$\Gamma(\rho^+ \rightarrow \pi^+ 3\pi^0)$ , and  $\Gamma(\rho^+ \rightarrow 2\pi^+\pi^-\pi^0)$ , the  $e^+e^- \rightarrow \pi^+\pi^-\pi^+\pi^-$  reaction cross section as a function of incident energy (excitation curve) and compared it to the CMD-2 data [2] from Novosibirsk.

With respect to the role of the axial-vector meson  $a_1(1260)$  in the four-pion decays of  $\rho^0$ , the situation is somewhat controversial. On one side, the intermediate states containing the  $a_1(1260)$  were either ignored [9–13] or shown [11] to have little influence on the four-pion decay widths of  $\rho(770)$ <sup>1</sup>. On the other side, the analysis of the differential distributions of charged pions coming from the  $e^+e^-$  annihilation in the energy range 1.05–1.38 GeV demonstrated the dominance of the  $a_1(1260)\pi$  intermediate states [14]. Given the large width of  $a_1(1260)$  ( $\Gamma_{a_1}=250$  to 600 MeV [15]) it would be surprising if the role of the  $a_1$ -meson diminished so fast outside the above range, which is not too far from the  $\rho(770)$  mass. Moreover, the  $a_1(1260)$  meson was shown to be important in the four-pion decays of the  $\tau$ -lepton [4, 16, 17], which are in a sense isospin counterparts of the four-pion final states in the  $e^+e^-$  annihilation. Recently, the paper of Achasov and Kozhevnikov has appeared [18] that included the intermediate states with the  $a_1$  meson using the generalized hidden local symmetry model [19]. This increased the  $\rho^0 \rightarrow 2\pi^+2\pi^-$  decay width from 0.94 keV to 1.59 keV assuming the nominal mass of the  $a_1$  resonance, see Table I in [18]. Unfortunately, the authors of [18] do not provide the comparison with the  $e^+e^- \rightarrow 2\pi^+2\pi^-$  cross section, which has a greater discriminatory value than the decay width alone [12, 13].

The present work was triggered by our interest in the electromagnetic probes in relativistic heavy-ion collisions. The production of prompt dileptons and photons is for a long time considered a powerful tool for investigating the properties of dense systems created in the hadronic and nuclear collisions [20, 21]. The interest of the heavy ion community in dilepton production has recently been boosted by very precise dimuon data by the CERN/NA60 collaboration [22]. The prompt dileptons and photons can, in principle, originate from two sources: (i) quark-gluon plasma, (ii) hadron gas. The theoretical calculations of the dilepton and photon yield from the latter are hampered by not uniquely known Lagrangian of the  $a_1\rho\pi$  interaction [23, 24]. We suggest one way how to relieve this problem and make the predictions of the dilepton and photon production from hadron gas more reliable. The results of the present work have already been utilized [25] in the evaluation of the dimuon production rate in In-In collisions at 158 A GeV.

A way of narrowing the uncertainty interval in dilepton production from the hadron gas was advocated a long time ago by Li and Gale [26]. They checked the feasibility of the dilepton rate calculation in, e.g.,  $\omega\pi^0$  collisions, by comparing the inverse process ( $e^+e^-$  annihilation into the  $\omega\pi^0$  final state) with the available experimental data. Li and Gale also considered the  $e^+e^-$  annihilation into four pions in the narrow  $a_1$  width approximation, i.e. as process  $e^+e^- \rightarrow a_1\pi$ . In the present work we handle it as a genuine four-final-pion process, considering not only the  $a_1\pi$  intermediate states but also other intermediate states following from various models based on the chiral perturbation theory.

In this paper we investigate the role of the  $a_1(1260)$  resonance in the  $e^+e^-$  annihilation into four charged pions and in the four-charged-pion decays of  $\rho(770)$  in more detail. We supplement three existing models, which consider only  $\rho$  and  $\pi$  in intermediate states (diagrams (a) and (b) in Fig. 1), with the  $a_1$  contribution (diagrams (d) in Fig. 1). Those three models are (1) the model of Eidelman, Silagadze, and Kuraev [10], (2) one of the models considered by Plant and Birse [11], and (3) the model of Achasov and Kozhevnikov [12, 13]. We will consider only the final state with all charged pions, for which the experimental data are best. The difference between the approach of Achasov and Kozhevnikov [18] and ours lies mainly in the  $a_1\rho\pi$  Lagrangian. In [18], the generalized hidden local symmetry Lagrangian was chosen, whereas we choose a more phenomenological two-term Lagrangian, which is often used in a different branch of the particle physics. Its individual terms and their specific combinations appeared in many papers computing the dilepton and photon production rate from a thermalized meson gas. In this paper we consider the mixing angle between the two terms as a free parameter and will determine its value by fitting the excitation curve of the  $e^+e^- \rightarrow \pi^+\pi^-\pi^+\pi^-$  reaction.

In order to evaluate the amplitude induced by eight diagrams Fig. 1(d) we have to choose a Lagrangian of the  $a_1\rho\pi$  interaction. For this choice, there are basically two approaches in the literature. One explores well defined theoretical concepts to build dynamical models, the free parameters of which are then fixed by comparison with observed masses and decay widths. See, e.g., Refs. [23, 27–34].

In other, more phenomenological, approaches the authors simply chose for the  $a_1\rho\pi$  Lagrangian various expressions built from the field operators and compatible with the fundamental conservation laws. Such Lagrangians, after fixing their coupling constants, were then used to calculate various observable quantities, see, e.g., [35–38]. In some approaches [5, 39], directly the vertex factors were written without showing the corresponding Lagrangian. From the fact that different authors pick different Lagrangians one might get the impression that the choice of Lagrangian is

---

<sup>1</sup> Ecker and Unterdorfer [7, 8] also included the  $a_1$  contribution when calculated the  $\rho^0 \rightarrow 4\pi$  branching fractions, but it is impossible for us to assess its role because they did not show results without it.

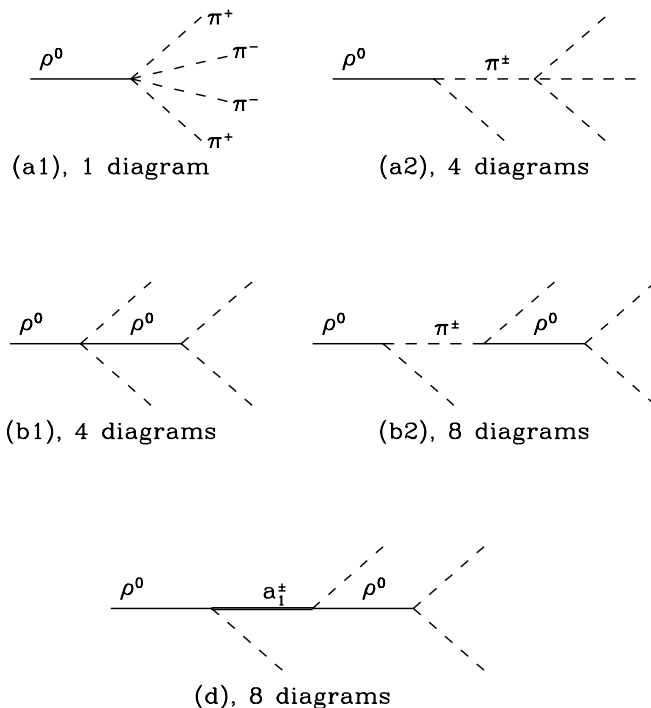


FIG. 1: Selected Feynman diagrams describing decay  $\rho^0 \rightarrow \pi^+ \pi^- \pi^+ \pi^-$

not very important and that various Lagrangians lead to identical, or at least similar, results. This is not true, and the observable quantities may be very sensitive to the choice of the  $a_1 \rho \pi$  Lagrangian, as was demonstrated, e.g., by Song [23]. The discussion of the  $a_1$  phenomenology with emphasis on the photon and dilepton production from a hot meson gas can be found in Ref. [24].

With so many  $a_1 \rho \pi$  effective Lagrangians, it is interesting to learn which Lagrangian is preferred experimentally. This would require constructing a general Lagrangian with a set of free parameters and fixing them by comparing all possible observables with the existing data. Of course, such a program is very ambitious. In this paper we are going to do something much simpler. Below, we choose a two-component Lagrangian and determine its two free parameters by requiring that the decay width of  $a_1(1260)$  be reproduced and the best possible fit obtained for the excitation curve of the  $e^+ e^- \rightarrow \pi^+ \pi^- \pi^+ \pi^-$  reaction. Even this restricted program cannot be accomplished completely. Firstly, the width of  $a_1(1260)$  is not known reliably. We will consider three values from the range given in the Particle Data Group tables [15], namely 250, 400, and 600 MeV. Secondly, the result of the fit will depend also on the basic  $\rho$  and  $\pi$  intermediate state model to which we add the  $a_1 \pi$  contribution. Nevertheless, we will show that the inclusion of the  $a_1 \pi$  intermediate states is necessary for obtaining good agreement with the  $e^+ e^- \rightarrow \pi^+ \pi^- \pi^+ \pi^-$  excitation curve.

Following the suggestion of T. Barnes [40] we also include the ratio of the  $D$ -wave and  $S$ -wave amplitudes of the  $a_1 \rightarrow \rho \pi$  decay as a fitted quantity. The importance of the  $D/S$  ratio for selecting among the  $a_1 \rho \pi$  Lagrangians was stressed in a different context in [24]. We use the experimental value  $D/S = -0.14 \pm 0.11$  [41], which was obtained by genuine partial wave analysis of the reaction  $\pi^- p \rightarrow \pi^+ \pi^- \pi^- p$ . We consider the other values which exist in literature strongly model biased. They were obtained by fitting the three-pion mass spectrum in the decay  $\tau \rightarrow \nu_\tau 3\pi$  using the model of Isgur, Morningstar, and Reader [5] and then calculating the  $D/S$  ratio from the optimal parameters of the model.

## II. ORIGINAL MODELS, MODIFICATIONS, AND ADDITIONS

As we already stated, we will complement three existing models of the four-pion decays, which consider only intermediate states with  $\rho$  mesons and pions, with the intermediate states containing the axial-vector resonance  $a_1(1260)$ . We must admit that our choice of models is rather arbitrary. Moreover, we took the models as they appeared in the literature and did not check their compatibility with chiral symmetry and with the constraints on coupling of resonances to the pions [42, 43].

Those three models are characterized below.

### A. Model of Eidelman, Silagadze, and Kuraev (ESK)

This model [10] is based on the effective chiral Lagrangian by Brihaye, Pak, and Rossi [44], which was investigated also in [45]. It follows from that Lagrangian that all (a) and (b) diagrams depicted on Fig. 1 contribute to the  $\rho^0 \rightarrow \pi^+\pi^-\pi^+\pi^-$  decay rate. Their amplitudes (in the notation slightly different from ours) are shown in the paper. Our usage of this model will differ from the original paper in three respects: (1) We add  $a_1$  diagrams Fig. 1(d). (2) We use a different value of the parameter  $\alpha_k$ , defined in [10]. Instead of 0.55 we set  $\alpha_k = 0.5$ , which follows from the KSFR relation [46], to be in conformity with other two models. (3) We replace the scalar part of the  $\rho$ -meson propagator with fixed mass and fixed width by the prescription

$$P_\rho(s) = -\frac{i}{s - M_\rho^2(s) + im_\rho\Gamma_\rho(s)}, \quad (2.1)$$

which uses the running mass squared  $M_\rho^2(s)$  and the energy dependent total width  $\Gamma_\rho(s)$  from Ref. [47].

The last point deserves more comments. The denominator of our propagator (2.1) is an analytic function in the  $s$ -plane with a cut running from  $4m_\pi^2$  to infinity, as required by general principles. This property differs (2.1) from most of the formulas used in the literature. The real function  $M_\rho^2(s)$  is calculated from  $\Gamma_\rho(s)$  using a once subtracted dispersion relation, which guarantees that the condition  $M_\rho^2(m_\rho^2) = m_\rho^2$  is satisfied. Further condition

$$\left. \frac{dM_\rho^2(s)}{ds} \right|_{s=m_\rho^2} = 0 \quad (2.2)$$

is not fulfilled automatically and serves as a test that all important contributions to the total  $\rho$ -meson width  $\Gamma_\rho(s)$  have properly been taken into account. See [47] for details. If we replace the  $m_\rho$  accompanying  $\Gamma_\rho(s)$  in Eq. (2.1) by  $\sqrt{s}$ , as it is done in some existing formulas, the condition (2.2) cannot be satisfied for any reasonable choice of  $\Gamma_\rho(s)$ .

The running mass approach [47] takes into account, in addition to the basic two-pion decay channel, several channels ( $\omega\pi^0$ ,  $K^+K^-$ ,  $K^0\bar{K}^0$ , and  $\eta\pi^+\pi^-$ ) which open as the  $\rho$  resonance goes above its nominal mass. It also considers structure effects described by the strong form factors. In these two respects it differs from other approaches that appeared in the literature [48–50]. Gounaris and Sakurai [48] considered only the two-pion contribution to the total width of the  $\rho^0$  resonance and ignored structure effects. Vaughn and Wali [49] took into account the strong form factor, but again ignored higher decay channels. Melikhov, Nachtmann, Nikonov, and Paulus [50] included the  $K^+K^-$  and  $K^0\bar{K}^0$  channels, but did not consider the strong form factors.

We will use the  $\rho$  propagator (2.1) not only in conjunction with the ESK model, but also with the other ones. This is the main reason why our results calculated within the original models (i.e., without the  $a_1\pi$  intermediate states) and presented below differ slightly from the results quoted in the original papers.

### B. One of the models of Plant and Birse (PB/HG)

Plant and Birse [11] investigated several models of the four-pion decays of  $\rho^0(770)$ . One of them (labeled HG) is a corrected version of the model by Bramon, Grau, and Pancheri [9], which was based on the hidden gauge theory of Bando *et al.* [51]. The  $2\pi 2\rho$  contact terms, see diagram (b1) in Fig. 1, are missing in this approach. The amplitude of the (a1) diagram is different from that in work by Eidelman, Silagadze, and Kuraev [10] by a factor  $(-1/2)$ . The amplitudes of (a2) and (b2) diagrams are equal to their ESK counterparts.

### C. Model of Achasov and Kozhevnikov (AK)

Achasov and Kozhevnikov [12, 13] studied the four-pion decays of  $\rho(770)$ , five-pion decays of  $\omega(782)$ , and the processes related to them. Namely, the  $e^+e^-$  annihilation into the four- and five-pion final states and the four-pion decays of the  $\tau$  lepton. They used the Weinberg Lagrangian [52] obtained upon the nonlinear realization of chiral symmetry. From their rather extensive work we adopt their prescriptions for the amplitudes (a1), (a2), and (b2) of the  $\rho^0 \rightarrow \pi^+\pi^-\pi^+\pi^-$  decay. The contact amplitude (b1) is again vanishing. Achasov and Kozhevnikov used a fixed-mass, variable-width formula for the  $\rho$ -meson propagator.

### D. $a_1\rho\pi$ Lagrangian and the amplitude of the diagrams containing the $a_1$ meson

We choose the following interaction among the  $a_1$ ,  $\rho$ , and  $\pi$  fields

$$\mathcal{L} = \frac{g_{a_1\rho\pi}}{\sqrt{2}} (\mathcal{L}_1 \cos\theta + \mathcal{L}_2 \sin\theta), \quad (2.3)$$

where  $g_{a_1\rho\pi}$  and  $\theta$  are yet undetermined parameters,

$$\mathcal{L}_1 = \mathbf{A}^\mu \cdot (\mathbf{V}_{\mu\nu} \times \partial^\nu \phi), \quad (2.4)$$

$$\mathcal{L}_2 = \mathbf{V}_{\mu\nu} \cdot (\partial^\mu \mathbf{A}^\nu \times \phi), \quad (2.5)$$

and  $\mathbf{V}_{\mu\nu} = \partial_\mu \mathbf{V}_\nu - \partial_\nu \mathbf{V}_\mu$ . The isovector composed of the  $\rho$ -meson field operators is denoted by  $\mathbf{V}_\mu$ , similar objects for  $\pi$  and  $a_1$  are  $\phi$  and  $\mathbf{A}^\mu$ , respectively. We write

$$\begin{aligned} \phi_1 &= \frac{1}{\sqrt{2}} (\phi_c + \phi_c^\dagger), \\ \phi_2 &= \frac{i}{\sqrt{2}} (\phi_c - \phi_c^\dagger), \\ \phi_3 &= \phi_n, \end{aligned}$$

and assume that  $\phi_c$  contains the annihilation operators of the positive pion and creation operators of the negative pion.  $\phi_n$  is the operator of neutral pion field.

A specific combination of terms (2.4) and (2.5) appeared in the pioneering work by Wess and Zumino [27]. Term (2.4) alone was used by Xiong, Shuryak, and Brown [39] in their study of the photon production from meson gas. Janssen, Holinde, and Speth [37] picked the term (2.5) when they evaluated the amplitude of the  $\pi\rho$  scattering. Another combination of (2.4) and (2.5) appeared in the calculation of dilepton production from meson gas by Song, Ko, and Gale [53].

Lagrangian (2.3) leads to the following factor for the vertex in which an incoming  $a_1^+$  (index  $\alpha$ ), an outgoing  $\rho^0$  (index  $\mu$ ), and an outgoing  $\pi^+$  meet

$$\begin{aligned} V^{\alpha\mu}(p_{a_1}, p_\rho, p_\pi) &= \frac{g_{a_1\rho\pi}}{\sqrt{2}} \{ \cos\theta [p_\rho^\alpha p_\pi^\mu - (p_\pi p_\rho) g^{\alpha\mu}] \\ &\quad - \sin\theta [p_\rho^\alpha p_{a_1}^\mu - (p_{a_1} p_\rho) g^{\alpha\mu}] \}. \end{aligned} \quad (2.6)$$

The  $a_1^- \rho^0 \pi^-$  vertex acquires an extra minus sign. The evaluation of the decay rate of  $a_1^+ \rightarrow \rho^0 \pi^+$  using vertex (2.6) is straightforward.

$$\begin{aligned} \Gamma_{a_1^+ \rightarrow \rho^0 \pi^+} &= \frac{g_{a_1\rho\pi}^2}{192\pi m_{a_1}^3} \lambda^{1/2}(m_{a_1}^2, m_\rho^2, m_{\pi^+}^2) \\ &\quad \times R(m_{a_1}^2, m_\rho^2, m_{\pi^+}^2), \end{aligned} \quad (2.7)$$

where

$$\lambda(x, y, z) = x^2 + y^2 + z^2 - 2xy - 2xz - 2yz$$

and

$$\begin{aligned} R(x, y, z) &= \left[ (x - y - z)^2 + \frac{y}{2x} (x - y + z)^2 \right] \cos^2 \theta \\ &\quad - 2 [(x - z)^2 + y(x + z - 2y)] \cos \theta \sin \theta \\ &\quad + [(x + y - z)^2 + 2xy] \sin^2 \theta. \end{aligned}$$

If we assume the charge independent  $a_1\rho\pi$  coupling constant and masses of  $\rho$  and  $a_1$ , the width of the decay  $a_1^+ \rightarrow \rho^+ \pi^0$  is obtained from (2.7) by changing just the pion mass. Formula

$$\Gamma_{a_1^+} = \Gamma_{a_1^+ \rightarrow \rho^0 \pi^+} + \Gamma_{a_1^+ \rightarrow \rho^+ \pi^0} \quad (2.8)$$

enables us to find the coupling constant  $g_{a_1\rho\pi}$  for given  $\Gamma_{a_1^+}$  and  $\sin\theta$ . Because each of the diagrams Fig. 1(d) contains two  $a_1\rho\pi$  vertices, the overall sign of the Lagrangian (2.3) is not important and we can assume a non-negative  $\cos\theta$ .

A question arises whether the narrow  $\rho$ -width approximation used above is accurate enough for the purpose of determination the  $g_{a_1\rho\pi}$  coupling constant. Achasov and Kozhevnikov [18] showed that the  $a_1$  decay width calculated as  $\Gamma(a_1 \rightarrow \rho\pi)$  came out larger than that calculated as  $\Gamma(a_1 \rightarrow 3\pi)$  using the same coupling constant  $g_{a_1\rho\pi}$ . We have examined this issue, too, using our two-component Lagrangian (2.3) and got that the  $\Gamma(a_1 \rightarrow 3\pi)/\Gamma(a_1 \rightarrow \rho\pi)$  ratio is smaller than unity (like in [18]) for  $\sin\theta \lesssim 0.2$  and  $\sin\theta \gtrsim 0.65$ . In the remaining interval, which contains all the values of  $\sin\theta$  that will be met in our calculations, this ratio is greater than one. Moreover, we have found that if one takes into account the strong form factors in the  $a_1\rho\pi$  and  $\rho\pi\pi$  vertices, the results of both approaches become almost identical. This can be explained as follows. According to Kokoski and Isgur [54] formula, which will be shown later, the strong form factor in a particular decay vertex is a decreasing function of the three-momentum of an outgoing particle in the rest frame of the parent particle. In the  $a_1 \rightarrow 3\pi$  decay the intermediate mass of  $\rho$  is mostly smaller than its nominal mass, what means higher momenta of particles emerging from the  $a_1\rho\pi$  vertex. In addition, the  $a_1 \rightarrow 3\pi$  width is further reduced by the form factor in the  $\rho\pi\pi$  vertex.

Let us now turn to the amplitude of the  $a_1$  diagrams Fig. 1(d) for the decay  $\rho^0(p) \rightarrow \pi^-(p_1)\pi^+(p_2)\pi^+(p_3)\pi^-(p_4)$ . We first introduce the notation

$$\begin{aligned} q_i &= p - p_i, \\ r_{ij} &= p_i + p_j, \\ s_{ij} &= r_{ij}^2, \end{aligned} \tag{2.9}$$

and then write the amplitude in the form

$$\mathcal{M}_d^{(\lambda)} = \epsilon_\lambda^\mu J_{d,\mu},$$

where  $\epsilon_\lambda^\mu$  is the polarization vector of the decaying  $\rho^0$  and

$$\begin{aligned} J_{d,\mu} &= -(1 - P_{12}P_{34})(1 + P_{14})(1 + P_{23})V_{\alpha\mu}(-q_4, -p, p_4) \\ &\times P_{a_1}^{\alpha\beta}(q_4)V_{\beta\nu}(q_4, r_{12}, p_3)g_\rho(p_2 - p_1)^\nu P_\rho(s_{12}). \end{aligned}$$

Here,  $P_{ij}$  denotes the operator that interchange four-momenta  $p_i$  and  $p_j$ . The axial-vector meson propagator

$$P_{a_1}^{\alpha\beta}(q) = i \frac{-g^{\alpha\beta} + \frac{1}{m_{a_1}^2} q^\alpha q^\beta}{q^2 - m_{a_1}^2 + im_{a_1}\Gamma_{a_1}} \tag{2.10}$$

is chosen in a simple fixed-mass, fixed-width form. Here, we are going to consider the four-pion system with invariant energies less than 1 GeV. The invariant mass of the three-pion system, which is equal to  $\sqrt{q^2}$ , is thus limited by 0.86 GeV. Achasov and Kozhevnikov [18] showed that the  $a_1$  decay width is negligible in that energy range. Referring to their finding we set  $\Gamma_{a_1} = 0$  in Eq. (2.10). The scalar part of the  $\rho$  propagator is again used in the form (2.1).

### E. Technicalities

The complete amplitude of the  $\rho^0 \rightarrow \pi^+\pi^-\pi^+\pi^-$  decay is

$$\mathcal{M}^{(\lambda)} = \epsilon_\lambda^\mu J_\mu, \tag{2.11}$$

where  $\epsilon_\lambda^\mu$  is the polarization vector of the decaying  $\rho^0$  and

$$J_\mu = J_{a,\mu} + J_{b,\mu} + J_{d,\mu}.$$

Four-vectors  $J_{a,\mu}$  and  $J_{b,\mu}$  describe the contributions from (a) and (b) diagrams in a particular model and  $J_{d,\mu}$  is the contribution from (d) diagrams. The sum over the  $\rho$ -meson polarizations of the amplitude (2.11) squared is given by

$$\sum_\lambda \left| \mathcal{M}^{(\lambda)} \right|^2 = \left( -g^{\mu\nu} + \frac{p^\mu p^\nu}{m_\rho^2} \right) J_\mu J_\nu^*. \tag{2.12}$$

This formula is more complicated than that used in [10], because the four-vectors  $J_{a,\mu}$  and  $J_{b,\mu}$  of PB/HG and AK models do not satisfy the transversality condition  $J_\mu p^\mu = 0$ . We used the algebraic manipulation program REDUCE [55] to express the sum (2.12) in terms of six invariants  $s_{ij}$ ,  $i < j$ ,  $j = 2, 3, 4$  defined in (2.9). Of course, only five of

them are independent and we used the identity  $\sum_{i<j} s_{ij} = m_\rho^2 + 8m_\pi^2$  for the checks in the process of evaluation of the decay width. When calculating the excitation curve,  $m_\rho^2$  is replaced by  $s$ , the square of the incident energy.

When calculating the decay width of an unpolarized parent particle, we may take advantage of the spherical symmetry of the problem and choose the following kinematic configuration: (1) The parent particle  $a$  is at rest. (2) The summed momentum  $\mathbf{p}_{12}$  of particles 1 and 2 points in the direction of the  $z$  axis. (3) The individual momenta  $\mathbf{p}_1$  and  $\mathbf{p}_2$  lie in the  $xz$  plane. Then the following formula, written in a general case with arbitrary masses and spins, is valid

$$\begin{aligned} \Gamma = & \frac{N}{16(2\pi)^6 m_a^2} \int_{m_1+m_2}^{m_a-m_3-m_4} dm_{12} p_1^* \int_{m_3+m_4}^{m_a-m_{12}} dm_{34} \\ & \times p_{12} p_3^* \int_{-1}^1 d\cos\theta_1^* \int_{-1}^1 d\cos\theta_3^* \int_0^{2\pi} d\varphi_3 |\overline{\mathcal{M}}|^2. \end{aligned} \quad (2.13)$$

The last quantity is the amplitude squared, averaged over the initial spin states, and summed over the final spin states. The factor  $N$  takes into account the identity of the final particles and equals  $1/4$  in our case. The asterisk denotes the momentum in the corresponding rest frame (1-2 or 3-4),  $p = |\mathbf{p}|$ , and  $m_{ij} = \sqrt{s_{ij}} = \sqrt{(p_i + p_j)^2}$ .

For evaluation of the integrals in (2.13) we used a sequence of the five one-dimensional Gauss-Legendre quadratures of the sixteenth order. We prefer this method to Monte-Carlo integration because we use the result of the integration in a minimization procedure and therefore we require that the same value of the optimized variable (Lagrangian mixing angle) yield always the same value of the minimized function, which would not be satisfied with the Monte-Carlo integration. Nevertheless, we checked our computer code by evaluating the decay width for a particular value of the mixing angle using a completely independent code based on the Monte-Carlo method.

To convert the calculated decay width into the cross section, we start with the formula

$$\sigma_{4\pi}(s) = \frac{\sigma_{\pi^+\pi^-}(s)}{\Gamma_{\pi^+\pi^-}(s)} \Gamma_{4\pi}(s).$$

Using

$$\sigma_{\pi^+\pi^-}(s) = \frac{\pi\alpha^2}{3s} \left(1 - \frac{4m_\pi^2}{s}\right)^{3/2} |F_\pi(s)|^2,$$

where  $F_\pi(s)$  is the contribution of the  $\rho$  resonance to the pion form factor, and

$$\Gamma_{\pi^+\pi^-}(s) = \frac{g_\rho^2 W}{48\pi} \left(1 - \frac{4m_\pi^2}{s}\right)^{3/2}$$

with  $W = \sqrt{s}$ , we arrive at

$$\sigma_{4\pi}(s) = \left(\frac{4\pi\alpha}{g_\rho}\right)^2 \frac{1}{W^3} |F_\pi(s)|^2 \Gamma_{4\pi}(s). \quad (2.14)$$

We further use the VMD expression for the dielectron decay width of  $\rho^0$

$$\Gamma_{e^+e^-} = \frac{4\pi m_\rho}{3} \left(\frac{\alpha}{g_\rho}\right)^2 \quad (2.15)$$

and get

$$\sigma_{4\pi}(s) = \frac{12\pi\Gamma_{e^+e^-}}{m_\rho W^3} |F_\pi(s)|^2 \Gamma_{4\pi}(s). \quad (2.16)$$

If we set, following Achasov and Kozhevnikov [13],

$$F_\pi(s) = \frac{m_\rho^2}{D_\rho(s)}, \quad (2.17)$$

where the inverse  $\rho$ -meson propagator  $D_\rho(s)$  is defined in Eq. (2.2) of [13], we reproduce their Eq. (3.1).

TABLE I:  $\chi^2/\text{NDF}$  of the fits to the CMD-2 cross section data (11 data points)

$\Gamma_{a_1}$ (MeV)	ESK [10]	PB/HG [11]	AK [12, 13]	only $a_1$
250	1.60	1.34	1.28	1.68
400	1.53	1.37	1.30	1.82
600	1.61	1.41	1.31	1.94
Only $\rho, \pi$	17.6	15.0	14.8	/

In our opinion, Eq. (2.16) overestimates the cross section if the experimental value of  $\Gamma_{e^+e^-}$  is used. The reason is that the dielectron decay width calculated from (2.15) is smaller than the experimental value. We will therefore stick with formula (2.14).

We utilize the scalar part of the  $\rho$ -meson propagator (2.1) to write our Ansatz for the  $\rho$ -meson contribution to the pion form factor

$$F_\pi(s) = \frac{M_\rho^2(0)}{M_\rho^2(s) - s - im_\rho\Gamma_\rho(s)}. \quad (2.18)$$

As shown in [47], this formula gives the correct value of the mean square radius of the pion. The form factor (2.17) fails in this test.

For the  $\rho$  coupling constant we use the same value as in [11–13], namely  $g_\rho = 5.89$ . This value is compatible with what follows from the KSRF relation [46] ( $5.900 \pm 0.011$ ). Both values are little lower than  $g_\rho = 6.002 \pm 0.015$  calculated from the  $\rho$ -meson width.

### III. LOW-ENERGY RESULTS ( $W < 1$ GeV)

We deal with the excitation curves of the reaction  $e^+e^- \rightarrow \pi^+\pi^-\pi^+\pi^-$  calculated in three different models (ESK, PB/HG, AK) supplemented with the  $a_1$  diagrams Fig. 1(d). We first fit them to the CMD-2 data [2] by varying the sine of the mixing angle  $\theta$ , defined in (2.3), for the three fixed values of the width of the  $a_1(1260)$  meson. We did not consider the first two points in the CMD-2 data, because they give only upper bounds of the cross section. The ratios of the usually defined  $\chi^2$  to the number of degrees of freedom (NDF), which characterize the quality of the fit, are shown in Table I. The last row in Table I shows the values of  $\chi^2/\text{NDF}$  that indicate how well (or badly) the original models without  $a_1$  agree with the data. No free parameter is involved in the latter case. Table I shows that the ratio  $\chi^2/\text{NDF}$  is always greater than one. In what follows, we shall therefore multiply the statistical errors of the quantities obtained in the process of minimization by the square root of that ratio.

The inspection of Table I shows that the inclusion of the  $a_1$  contribution greatly improves the agreement with the data. The interference between the original diagrams and the new ones is important, the results of the combined model are better than those of the  $a_1$  diagrams alone. The best results (lowest  $\chi^2$ ) are obtained with the AK model supplemented with the  $a_1\pi$  intermediate states.

To investigate the sensitivity of our results to the input data, we combine the CMD-2 data [2] and the low-energy ( $s < 1$  GeV<sup>2</sup>) part of the BaBar data [56] (BaBar-LE in what follows) into a new set and repeat the calculations. The results are shown in Table II. Their comparison with the results obtained from the CMD-2 data alone shows two important differences: (i) The agreement of all models with data, characterized by  $\chi^2/\text{NDF}$ , is now better. It indicates that the CMD-2 and BaBar-LE data are compatible, so the increased number of data points does not bring proportional increase of  $\chi^2$ . (ii) Whereas merging of the  $a_1$  diagrams with the PB/HG or AK model improves the fit, adding the ESK model diagrams to the pure  $a_1$  contribution leads to the opposite effect.

Next, we add the  $D/S$  ratio [41] to the set of fitted experimental values and repeat the calculations. The results are shown in Table III. The salient feature of those results is a clear preference of the highest assumed value (600 MeV) of the total  $a_1$  width.

In Figs. 2, 3, and 4 we show the comparison of the combined set of data with the excitation curves calculated in all three models supplemented with the  $a_1$  diagrams Fig. 1(d). The same comparison for the  $a_1$  diagrams alone is depicted in Fig. 5.

In Table IV we can see the values of  $\sin\theta$  together with their errors (defined in the usual way [57]) obtained from the fit to the CMD-2 & BaBar-LE cross section data and to the  $D/S$  ratio. As we mentioned above, three different values of the  $a_1(1260)$  width are assumed. Table V compares the experimental value of the  $\rho^0 \rightarrow \pi^+\pi^-\pi^+\pi^-$  decay



TABLE II:  $\chi^2/\text{NDF}$  of the fits to the combined CMD-2 & BaBar-LE cross section data (27 data points)

$\Gamma_{a_1}$ (MeV)	ESK [10]	PB/HG [11]	AK [12, 13]	only $a_1$
250	1.42	1.20	1.19	1.32
400	1.48	1.21	1.18	1.39
600	1.55	1.22	1.19	1.44
Only $\rho, \pi$	9.4	10.4	10.3	/

TABLE III:  $\chi^2/\text{NDF}$  of the fits to the CMD-2 & BaBar-LE cross section data and to the  $D/S$  ratio (28 data points)

$\Gamma_{a_1}$ (MeV)	ESK [10]	PB/HG [11]	AK [12, 13]	only $a_1$
250	3.66	1.95	1.99	1.96
400	1.98	1.34	1.33	1.48
600	1.65	1.20	1.18	1.41

width [2] with the results obtained from various models under the same conditions. The results for both quantities obtained with other data sets (CMD-2 only, CMD-2 & BaBar-LE) are very similar.

#### IV. HIGH-ENERGY RESULTS (W UP TO 4.5 GeV)

When we want to get a good description of the data on the  $e^+e^-$  annihilation to four charged pions at energies above 1 GeV, we should consider also the contribution from diagrams where higher  $\rho$  resonances couple to the virtual photon and then convert into four pions. We include two resonances:  $\rho' = \rho(1450)$  and  $\rho'' = \rho(1700)$ . We assume that the decay of those resonances into four pions is governed by the same Feynman diagrams as that of  $\rho(770)$ , with all coupling constants scaled by the same factor (different for  $\rho'$  and  $\rho''$ ). This assumption implies that the four-pion

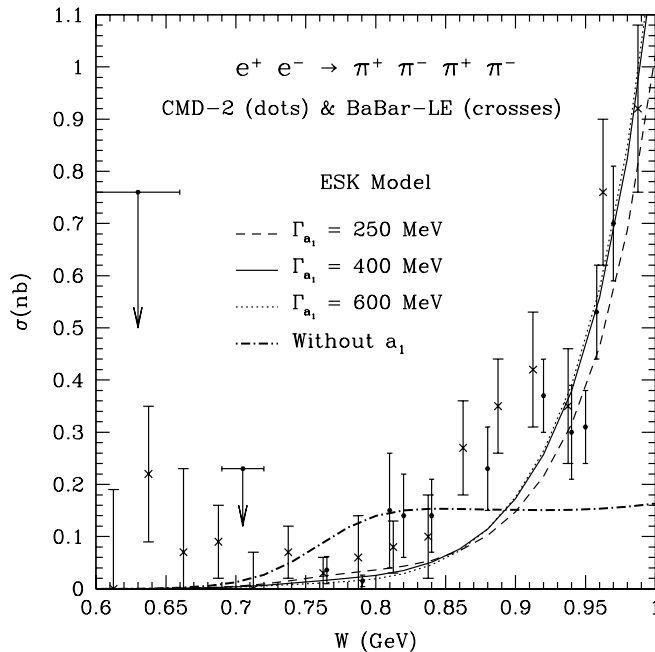


FIG. 2: Excitation curves calculated in the original (without  $a_1$  meson) and expanded ESK model compared to the CMD-2 and BaBar-LE data. The  $D/S$  ratio was also used in fit.

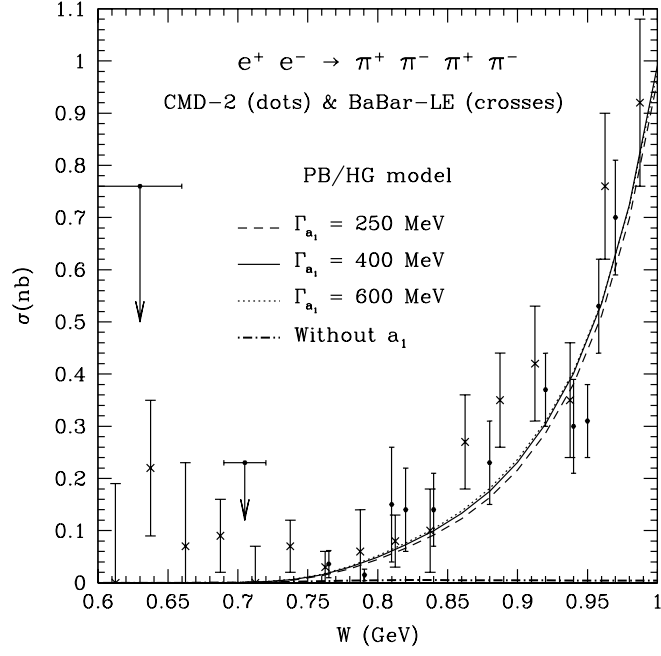


FIG. 3: Excitation curves calculated in the original (without  $a_1$  meson; dash-dotted curve close to the abscissa) and expanded PB/HG model compared to the CMD-2 and BaBar-LE data. The  $D/S$  ratio was also used in fit.

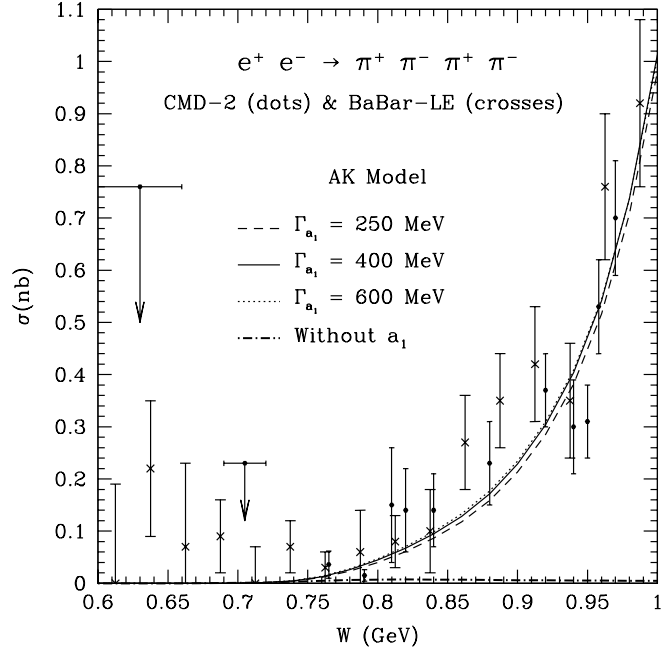


FIG. 4: Excitation curves calculated in the original (without  $a_1$  meson; dash-dotted curve close to the abscissa) and expanded AK model compared to the CMD-2 and BaBar-LE data. The  $D/S$  ratio was also used in fit.

TABLE IV: Values of  $\sin \theta$  from the fit to the CMD-2 & BaBar-LE data and to the  $D/S$  ratio.

$\Gamma_{a_1}$ (MeV)	ESK [10]	PB/HG [11]	AK [12, 13]	only $a_1$
250	0.4092(33)	0.4278(32)	0.4267(32)	0.4312(35)
400	0.4352(24)	0.4624(34)	0.4608(32)	0.4679(39)
600	0.4659(27)	0.5046(44)	0.5022(41)	0.5132(55)

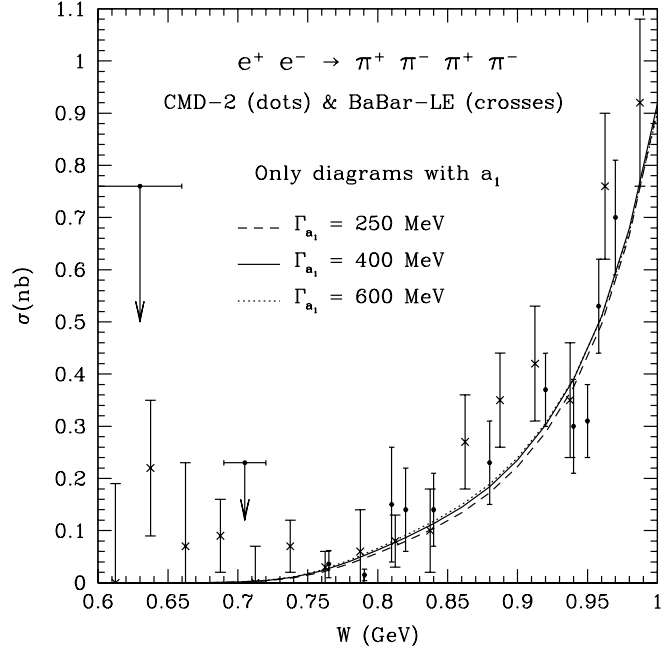


FIG. 5: Excitation curves calculated from the  $a_1\pi$  diagrams only, compared to the CMD-2 and BaBar-LE data. The  $D/S$  ratio was also used in fit.

TABLE V: Decay width  $\Gamma(\rho^0 \rightarrow \pi^+\pi^-\pi^+\pi^-)$  (keV) calculated in various models using  $\sin\theta$  from the fits to the CMD-2 & BaBar-LE data and to the  $D/S$  ratio. Experimental value is  $(2.8 \pm 1.4 \pm 0.5)$  keV [2].

$\Gamma_{a_1}$ (MeV)	ESK [10]	PB/HG [11]	AK [12, 13]	only $a_1$
250	4.28(01)	3.16(25)	2.70(23)	4.52(30)
400	2.81(01)	3.55(28)	3.03(26)	5.08(32)
600	1.94(02)	3.77(30)	3.22(27)	5.39(37)
Only $\rho, \pi$	16.2	0.59	0.89	/

decay widths of  $\rho'$  and  $\rho''$  have the same shape in  $W$  as that of  $\rho(770)$ . They only differ from it by constant factors. The simplifying assumption we have made allows us to use the same cross section formula (2.14) as in the low energy case, with  $F_\pi(s)$  replaced by

$$F(s) = F_\rho(s) + \delta F_{\rho'}(s) + \epsilon F_{\rho''}(s), \quad (4.1)$$

where  $F_\rho(s)$  differs from (2.18) by including also  $\Gamma_{\rho^0 \rightarrow \pi^+\pi^-\pi^+\pi^-}(s)$  into the total decay width of  $\rho(770)$ ,

$$F_{\rho'}(s) = \frac{m_{\rho'}^2}{m_{\rho'}^2 - s - im_{\rho'}\Gamma_{\rho'}}, \quad (4.2)$$

and similar expression holds also for  $F_{\rho''}(s)$ . Constants  $\delta$  and  $\epsilon$  not only include the coupling constants modification factors mentioned above, but also account for the fact that the couplings of  $\rho'$  and  $\rho''$  to photon differ from that of  $\rho(770)$ , which is fixed by VMD. Unknown complex parameters  $\delta$  and  $\epsilon$  will be determined, together with the masses and widths of  $\rho'$  and  $\rho''$  and other two parameters mentioned later on, by fitting the experimental excitation function<sup>2</sup>.

<sup>2</sup> When we replaced (2.18) by (4.1) in the low-energy region and kept the form-factor parameters as determined in the high-energy fit, we got the results that differed slightly from that in Sec. III. If we varied also those parameters when fitting the low-energy data, they acquired unphysical values (masses of  $\rho'$  and  $\rho''$  around 1 GeV). It may signify that some contribution important at low energies (scalar resonances) is still missing in our approach.

TABLE VI: Results of the fit to the BaBar cross section data and to the  $D/S$  ratio (145 data points) for  $\Gamma_{a_1} = 600$  MeV.

Model	ESK [10]	PB/HG [11]	AK [12, 13]	only $a_1\pi$
$\chi^2/\text{NDF}$	1.21	1.12	1.12	1.12
$\sin\theta$	0.4474(22)	0.4592(28)	0.4588(27)	0.4603(28)
$\beta$ (GeV)	0.3505(89)	0.3665(97)	0.3657(97)	0.3695(98)
$m_{\rho'}$ (GeV)	1.419(12)	1.439(13)	1.438(13)	1.442(13)
$\Gamma_{\rho'}$ (GeV)	0.564(20)	0.568(21)	0.568(21)	0.566(21)
$\text{Re}(\delta)$	0.1038(41)	0.1145(51)	0.1144(51)	0.1149(53)
$\text{Im}(\delta)$	-0.039(11)	-0.019(12)	-0.021(12)	-0.015(13)
$m_{\rho''}$ (GeV)	1.903(21)	1.923(24)	1.922(24)	1.926(24)
$\Gamma_{\rho''}$ (GeV)	0.247(38)	0.284(44)	0.283(44)	0.290(45)
$\text{Re}(\epsilon)$	-0.0016(11)	-0.0002(17)	-0.0003(17)	0.0002(18)
$\text{Im}(\epsilon)$	-0.00373(94)	-0.0054(12)	-0.0054(12)	-0.0056(13)

Another effect that has to be taken into account when dealing with higher energies is connected with the structure of the strongly interacting particles. Our decay amplitudes have been derived under the assumption that the pions,  $\rho$ 's, and  $a_1$ 's are elementary quanta of the corresponding quantum fields. But this assumption is justified only when their mutual interaction is soft. When the momenta of the mesons which enters a specific interaction vertex get higher, the contribution of that vertex to the amplitude becomes smaller than in the case of the point-like participants. This effect is usually described by strong form factors. Given the present status of the strong interaction theory, we have to turn to models. For example, in the chromoelectric flux-tube breaking model of Kokoski and Isgur [54], the vertex describing a two-body decay is modified by the factor  $\exp\{-p^{*2}/(12\beta^2)\}$ , where  $p^*$  is the three-momentum magnitude of the decay products in the parent particle rest frame and  $\beta \approx 0.4$  GeV. For decay of the  $\rho$  meson with a (non-nominal) mass  $W$  into two on-mass-shell pions, this form factor can be written as

$$F_{KI}(s) = \exp\left\{-\frac{s-s_0}{48\beta^2}\right\}, \quad (4.3)$$

where  $s = W^2$  and  $s_0$  is the threshold value of  $s$  ( $4m_\pi^2$  in the two-pion decay). The complete amplitude of the four-pion decay of  $\rho^0$  contains many vertices, some of them with more than three incoming/outgoing particles. Applying the Kokoski-Isgur factor to each of them would be cumbersome and would require additional assumptions in the case of more complicated vertices. We will therefore assign an ‘‘effective’’ strong form factor of the form (4.3) to the complete amplitude of the decay  $\rho^0 \rightarrow \pi^+\pi^-\pi^+\pi^-$ , but with  $s_0 = 16m_\pi^2$ . When fitting the experimental excitation curve,  $\beta$  will be considered as another parameter. With the masses and widths of  $\rho'$  and  $\rho''$ , complex parameters  $\delta$  and  $\epsilon$ , and with the sine of the mixing angle  $\theta$  there are ten real parameters to be determined by fitting the  $e^+e^- \rightarrow \pi^+\pi^-\pi^+\pi^-$  cross section data of BaBar collaboration [56].

In the following, we assume the  $a_1$  decay width of 600 MeV, for which the results of all models at energies below 1 GeV were best. The same value was used in the  $a_1$  propagator (2.10).

The resulting optimized values of the parameters listed above and their MINUIT [57] errors are shown in Table VI for the three different models supplemented with the  $a_1\pi$  intermediate states and for the latter alone. Mutual comparison of the  $\chi^2/\text{NDF}$  ratios clearly shows that the presence of the  $a_1\pi$  intermediate states is crucial for obtaining good agreement of the calculated excitation curve with data. They provide a good fit even if taken alone. Adding the diagrams with  $\pi$ 's and  $\rho$ 's in the intermediate states does not change the quality of the fit if their amplitudes are taken from the PB/HG and AK models. On the other hand, the inclusion of the amplitudes of the ESK model brings some deterioration of the fit. The values of parameter  $\beta$  do not differ very much from the value advocated in [54] for the three-line vertices, what indicates that the effective-strong-form-factor approach we have chosen (4.3) is reasonable. The values of the sine of the mixing angle  $\theta$  are somewhat lower than those at low energies. The central values of the masses and widths of  $\rho'$  and  $\rho''$  a little different from those listed in [15], but differences are acceptable keeping in mind relatively large errors.

The graphical comparison of the excitation curve calculated from the model containing only the diagrams with the  $a_1\pi$  intermediate states, shown in Fig. 1(d), with experimental data [56] is presented in Fig. 6. The excitation curves of other models (ESK, PB/HG, AK) combined with the  $a_1\pi$  contribution differ only slightly and are not shown.

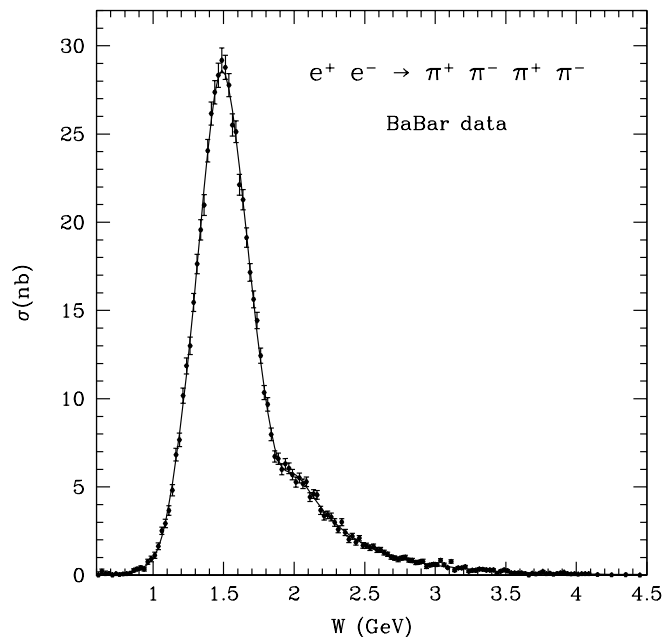


FIG. 6: Theoretical excitation curve compared with the BaBar data [56]. The  $D/S$  ratio was also used in fit. The result of the pure  $a_1$  model is shown. The other models combined with  $a_1\pi$  intermediate states provide almost identical curves.

## V. CONCLUSIONS AND COMMENTS

Our low-energy results show that the inclusion of the  $a_1\pi$  intermediate states is of vital importance for obtaining a good agreement with the experimental data on the cross section of the reaction  $e^+e^- \rightarrow \pi^+\pi^-\pi^+\pi^-$  as a function of the incident energy (see Tables I, II, and III or Figs. 2, 3, and 4). The  $\chi^2/\text{NDF}$  ratio gets much smaller if a particular model is supplemented with the diagrams containing the  $a_1$  resonance in the intermediate states. Viewing from another perspective, the pure  $a_1$  model provides relatively good agreement with the cross section data, much better than each of the three models without the  $a_1\pi$  intermediate states. See Tables mentioned above and Fig. 5. Adding the diagrams from the original models to the pure  $a_1$  model improves the fit in the case of the PB/HG and AK models, but worsens it in the case of the ESK model. Unfortunately, the  $\chi^2/\text{NDF}$  ratio remains greater than one everywhere. It may be the consequence of our ignoring some important contributions, perhaps those with a scalar resonance considered in [4, 6]. The original models ESK, PB/HG, and AK do not contain any scalar resonances. We also have not included them as our main concern was the role of the  $a_1$  resonance. It is also possible that the  $a_1\rho\pi$  Lagrangian should contain more terms than considered in (2.3).

Using the  $D/S$  ratio as an additional data point is important. It can discriminate among various models. In our case it increases the separation of the ESK model from the others. It also strongly prefers larger values of the assumed  $a_1$  width. In calculations without the  $D/S$  ratio we were able to find a value of  $\sin\theta$  for each  $\Gamma_{a_1}$  that led to an acceptable fit to the  $e^+e^- \rightarrow 2\pi^+2\pi^-$  cross section. However, the lowest value of  $\Gamma_{a_1}$  is excluded if we add the  $D/S$  ratio to the fitted data (see Table III).

As to the partial decay width of  $\rho^0 \rightarrow \pi^+\pi^-\pi^+\pi^-$ , the conclusion is not so categorical. Two models (PB/HG and AK) in their original forms provided results that were a little smaller, but did not contradict strongly the experimental value with its large errors. Only the original ESK model gave too large figure, which was in a clear disagreement with the experimental value. The inclusion of the  $a_1\pi$  intermediate states brought all values into the interval given by the experimental value and its errors summed linearly, see Table V. It must be said that the pure  $a_1$  model gives the decay widths that are close to the one-sigma upper limit or even beyond it.

We originally hoped that our study would tell us the form of the  $a_1\rho\pi$  Lagrangian. But with respect to the  $a_1\rho\pi$  Lagrangian, no clear picture can be inferred from the low-energy results yet. The optimal values of the sine of the mixing angle, see Table IV, are from a broad interval and depend not only on the choice of the original model to which the  $a_1$  diagrams are added, but also on the assumed value of the  $a_1$  width. The optimized values of  $\sin\theta$  squeeze into interval (0.40, 0.51).

The quality of the fit over the whole energy range of the BaBar experiment [56], as measured by the  $\chi^2/\text{NDF}$  ratio, seems to be better than that at low energies. But a more careful investigation in terms of the confidence level, which

TABLE VII: Survey of the mixing parameter  $\sin\theta$  for various versions of two-component  $a_1\rho\pi$  Lagrangian (2.3) that appeared in literature.

No.	$\sin\theta$	Reference
1	0	[38, 39]
2	0.2169	[23, 24, 53]
3	0.5582	[58]
4	0.6308	[23, 24, 59]
5	1	[37]
	0.40–0.51	our low-energy fits
	0.41–0.47	our all-energy fits

takes into account  $\chi^2$  and NDF separately, shows equal quality of those two fits. The values of  $\sin\theta$  are compatible with those found at low energies,  $\sin\theta \in (0.41, 0.47)$  (lower boundary is obtained from the fits where  $\Gamma_{a_1} = 250$  MeV was used). They occupy a narrower interval, what can be explained by lesser importance of sub-dominant diagrams with only  $\rho$  and  $\pi$  mesons in the intermediate states.

It is interesting to compare our estimates of the mixing parameter  $\sin\theta$ , defined in Eq. (2.3), with its values that have been used so far, see Table VII. The values in the first and fifth row simply reflect the fact that Lagrangians in Refs. [37–39] contained just one term. The remaining rows refer to various sets of four fundamental parameters ( $m_0$ ,  $g$ ,  $\sigma$ , and  $\xi$ ) of the model in which the vector and axial-vector mesons were included as massive Yang-Mills fields of the  $SU(2)\times SU(2)$  chiral symmetry [23]. The model built on previous works [28–30]. Our mixing parameter is related to the parameters  $\eta_1$  and  $\eta_2$  of that model, which can be expressed in terms of the four fundamental parameters using Eqs. (2.9) and (2.10) in [23]. The formula is very simple

$$\sin\theta = \frac{\eta_2}{\sqrt{\eta_1^2 + \eta_2^2}}.$$

In [23], the fundamental parameters of the massive Yang-Mills model were determined using the experimental values of the masses and width of the  $\rho$  and  $a_1$  mesons. This procedure is not unique, there are two solutions. The corresponding mixing parameter is shown in the second and fourth row of Table VII. Row 3 corresponds to an *ad hoc* choice of fundamental parameters made in [58]. Last two rows show the range of our results obtained from various models (ESK, PB/HG, AK) and various assumed values of  $\Gamma_{a_1}$  (250, 400, and 600 GeV). Unfortunately, there is no overlap with the rows above. The issue definitely requires more attention. The phenomenological models may be improved by including other intermediate states, perhaps those with scalar resonances. The parameters of the massive Yang-Mills model may be tuned by using richer experimental input ( $\Gamma(a_1 \rightarrow \pi\gamma)$  and  $D/S$  ratio as in [24, 32]) and more realistic formulas for relating theoretical parameters to experimental quantities, e.g., calculating the  $a_1$  width as  $a_1 \rightarrow 3\pi$  instead of  $a_1 \rightarrow \rho\pi$ .

Our failure to obtain a more precise value of the mixing angle of the  $a_1\rho\pi$  Lagrangian suggests that it is necessary to make a simultaneous fit to data about several physical processes. The natural candidates are the  $e^+e^-$  annihilation into various four-pion final states, the decay of the  $\tau$  lepton into neutrino and three or four pions, and the exclusive hadronic reactions of the type investigated, e.g., in [37].

### Acknowledgments

One of us (P. L.) is indebted to David Kraus for useful discussions. We thank Prof. T. Barnes for useful correspondence. This work was supported by the Czech Ministry of Education, Youth and Sports under contracts MSM6840770029, MSM4781305903, and LC07050.

- 
- [1] Y. Nambu, Phys. Rev. **106**, 1366 (1957); W. R. Frazer and J. R. Fulco, Phys. Rev. Lett. **2**, 365 (1959); J. J. Sakurai, Ann. Phys. (N.Y.) **11**, 1 (1960); Y. Nambu and J. J. Sakurai, Phys. Rev. Lett. **8**, 79 (1962); **8**, 191(E) (1962); M. Gell-Mann, D. Sharp, and W. Wagner, *ibid.* **8**, 261 (1962); J.J. Sakurai, *Currents and Mesons* (University of Chicago Press, Chicago, IL, 1969).
- [2] R. R. Akhmetshin *et al.*, Phys. Lett. B **475**, 190 (2000).

- [3] P. Lichard, *Acta Physics Slovaca* **49**, 215 (1999).
- [4] R. Decker, P. Heiliger, H. H. Jonsson, and M. Finkemeier, *Z. Phys. C* **70**, 247 (1996).
- [5] N. Isgur, C. Morningstar, and C. Reader, *Phys. Rev. D* **39**, 1357 (1989).
- [6] H. Czyż and J. H. Kühn, *Eur. Phys. J. C* (18), 497 (2001).
- [7] G. Ecker and R. Unterdorfer, *Eur. Phys. J. C* **24**, 535 (2002).
- [8] G. Ecker and R. Unterdorfer, *Nucl. Phys. B Proc. Suppl.* **121**, 175 (2003).
- [9] A. Bramon, A. Grau, and G. Pancheri, *Phys. Lett. B* **317**, 190 (1993).
- [10] S. I. Eidelman, Z. K. Silagadze, and E. A. Kuraev, *Phys. Lett. B* **346**, 186 (1995).
- [11] R. S. Plant and M. C. Birse, *Phys. Lett. B* **365**, 292 (1996).
- [12] N. N. Achasov and A. A. Kozhevnikov, *Phys. Rev. D* **61**, 077904 (2000).
- [13] N. N. Achasov and A. A. Kozhevnikov, *Phys. Rev. D* **62**, 056011 (2000).
- [14] R. R. Akhmetshin *et al.*, *Phys. Lett. B* **466**, 392 (1999).
- [15] W.-M. Yao *et al.*, *Journal of Physics G* **33**, 1 (2006).
- [16] A. E. Bondar, S. I. Eidelman, A. I. Milstein, and N. I. Root, *Phys. Lett. B* **466**, 403 (1999).
- [17] K. W. Edwards *et al.*, *Phys. Rev. D* **61**, 072003 (2000).
- [18] N. N. Achasov and A. A. Kozhevnikov, *Phys. Rev. D* **71**, 034015 (2005); *Yad. Fiz.* **69**, 314 (2006) [*Phys. Atom. Nucl.* **69**, 293 (2006)].
- [19] M. Bando, T. Fujiwara, and K. Yamawaki, *Prog. Theor. Phys.* **79**, 1140 (1988).
- [20] E. L. Feinberg, *Nuovo Cim. A* **34**, 391 (1976).
- [21] E. Shuryak, *Phys. Lett.* **78B**, 150 (1978); *Yad. Fiz.* **28**, 796 (1978) [*Sov. J. Nucl. Phys.* **28**, 1548 (1978)].
- [22] R. Arnaldi *et al.* (NA60 Collaboration), *Phys. Rev. Lett.* **96**, 162302 (2006).
- [23] C. Song, *Phys. Rev. C* **47**, 2861 (1993).
- [24] S. Gao and C. Gale, *Phys. Rev. C* **57**, 254 (1998).
- [25] J. Ruppert, C. Gale, T. Renk, P. Lichard, and J. I. Kapusta, arXiv:0706.1934.
- [26] G.-Q. Li and C. Gale, *Phys. Rev. Lett.* **81**, 1572 (1998); *Phys. Rev. C* **58**, 2914 (1998); *Nucl. Phys. A* **638**, 491C (1998).
- [27] J. Wess and B. Zumino, *Phys. Rev.* **163**, 1727 (1967).
- [28] H. Gomm, Ö. Kaymakçalan, and J. Schechter, *Phys. Rev. D* **30**, 2345 (1984).
- [29] B. R. Holstein, *Phys. Rev. D* **33**, 3316 (1986).
- [30] U. G. Meissner, *Phys. Rept.* **161**, 213 (1988).
- [31] N. Kaiser and U. G. Meissner, *Nucl. Phys. A* **519**, 671 (1990).
- [32] P. Ko and S. Rudaz, *Phys. Rev. D* **50**, 6877 (1994).
- [33] B. A. Li, *Phys. Rev. D* **52**, 5165 (1995).
- [34] J. Smejkal, E. Truhlík, and H. Göller, *Nucl. Phys. A* **624**, 655 (1997).
- [35] T. N. Pham, C. Roiesnel, and T. N. Truong, *Phys. Lett. B* **78**, 623 (1978).
- [36] J. H. Kühn and A. Santamaria, *Z. Phys. C* **48**, 445 (1990).
- [37] G. Janssen, K. Holinde, and J. Speth, *Phys. Rev. C* **49**, 2763 (1994).
- [38] K. Haglin, *Phys. Rev. C* **50**, 1688 (1994).
- [39] L. Xiong, E. Shuryak, and G. E. Brown, *Phys. Rev. D* **46**, 3798 (1992).
- [40] T. Barnes, private communication.
- [41] S. U. Chung *et al.* (BNL/E852 Collaboration), *Phys. Rev. D* **65**, 072001 (2002).
- [42] G. Ecker, J. Gasser, H. Leutwyler, A. Pich, and E. de Rafael, *Phys. Lett.* **223**, 425 (1989).
- [43] G. Ecker, J. Gasser, A. Pich, and E. de Rafael, *Nucl. Phys. B* **321**, 311 (1989).
- [44] Y. Brihaye, N. K. Pak, and P. Rossi, *Nucl. Phys. B* **254**, 71 (1985); *Phys. Lett. B* **164**, 111 (1985).
- [45] E. A. Kuraev and Z. K. Silagadze, *Phys. Lett. B* **292**, 377 (1992).
- [46] K. Kawarabayashi and M. Suzuki, *Phys. Rev. Lett.* **16**, 255 (1966); **16**, 384(E) (1966); Riazuddin and Fayyazuddin, *Phys. Rev.* **147**, 1071 (1966).
- [47] P. Lichard, *Phys. Rev. D* **60**, 053007 (1999).
- [48] G. J. Gounaris and J. J. Sakurai, *Phys. Rev. Lett.* **21**, 244 (1968).
- [49] M. T. Vaughn and K. C. Wali, *Phys. Rev. Lett.* **21**, 938 (1968).
- [50] D. Melikhov, O. Nachtmann, V. Nikonov, and T. Paulus, *Eur. Phys. J. C* **34**, 345 (2004).
- [51] M. Bando, T. Kugo, S. Uehara, K. Yamawaki, and T. Yanagida, *Phys. Rev. Lett.* **54**, 1215 (1985); M. Bando, T. Kugo, and K. Yamawaki, *Nucl. Phys. B* **259**, 493 (1985).
- [52] S. Weinberg, *Phys. Rev.* **166**, 1568 (1968).
- [53] C. Song, C. M. Ko, and C. Gale, *Phys. Rev. D* **50**, R1827 (1994).
- [54] R. Kokoski and N. Isgur, *Phys. Rev. D* **35**, 907 (1987).
- [55] A. C. Hearn, *Reduce User's Manual, Version 3.6*, The Rand Corporation, Santa Monica, July 1995. See also <http://www.reduce-algebra.com/>.
- [56] B. Aubert *et al.* (BaBar Collaboration), *Phys. Rev. D* **71**, 052001 (2005).
- [57] F. James and M. Roos, *Comput. Phys. Commun.* **10**, 343 (1975).
- [58] S. Turbide, R. Rapp, and C. Gale, *Int. J. Mod. Phys. A* **19**, 5351 (2004).
- [59] S. Turbide, R. Rapp, and C. Gale, *Phys. Rev. C* **69**, 014903 (2004).